Nonlinear gain and bistability in photonic crystal heterostructures with compositional and doping superlattices

Valerii K. Kononenko [a*], Marian Marciniak [b], and Dmitrii V. Ushakov [c]

[a] Stepanov Inst. of Physics NASB, Fr. Scorina Pr., 70, 220072 Minsk, Belarus;
[b] National Inst. of Telecommunications, Szachowa Str., 1, 04-894 Warsaw, Poland;
[c] Belarussian State Univ., Fr. Scorina Pr., 4, 220050 Minsk, Belarus

ABSTRACT

Optical properties of photonic crystal heterostructures with embedded *n–i–p–i* superlattices are studied. Nonlinear behavior of the transmission and reflection spectra near the defect mode is investigated. Self-consistent calculations of the output performance characteristics are performed using the transfer-matrix method and taking into account the gain saturation. Features and characteristic parameters of the nonlinear gain in active *n–i–p–i* layers are determined. Detail analysis of the gain saturation and accompanying nonlinear refraction effects is carried out for one-dimensional photonic crystal heterostructure amplifiers in the GaAs–GaInP system having at the central part an active "defect" from the doubled GaAs *n-i-p-i* crystal. The gain saturation in the active layers in the vicinity of the defect changes the index contrast of the photonic structure and makes worse the emission at the defect mode. Spectral bistability effect which can be exhibited in photonic crystal heterostructure amplifiers is predicted and the hysteresis loop and other attending phenomena are described. The bistability behavior and modulation response efficiency demonstrate the potential possibilities of the photonic crystal heterostructures with *n-i-p-i* layers as high-speed optical amplifiers and switches.

Keywords: Photonic crystal heterostructure, *n–i–p–i* superlattice, defect mode, transmission spectrum, gain saturation, spectral bistability, hysteresis, switching.

1. INTRODUCTION

At present, low-dimensional photonic structures are generally recognized as a natural foundation of the future high-capacity networks. In particular, the photonic band-gap structures seem promising for providing the increase of optical nonlinear response of a material in order to attain high efficiency of optical processes at rather small volume. Based on photonic crystals, different novel compact optical devices can be realized, including optical switches, single-mode lasers and amplifiers, light pulse compressors, and frequency converters. A powerful principle that could be explored to implement all-optical transistors, switches, logical gates, and memory elements is the conception of optical bistability. In the systems that display optical bistability, the output intensity is a strong nonlinear function of the input intensity and a hysteresis loop behavior manifests.

As a candidate for the active medium with large optical nonlinearities, *n–i–p–i* crystals or doping superlattices can be used [1, 2]. The nonlinear processes in the *n–i–p–i* superlattices are connected with (a) the filling or emptying of the energy states under optical excitation of the crystal, (b) redistribution of the energy levels at the change of the potential relief depth, (c) the shortening of the density state tails, which are related to the impurity concentration fluctuations, at the screening of the electrostatic potential by non-equilibrium current carriers, (d) change in the lifetime of current carriers due to changes in the overlap of the envelope wave functions of electrons and holes, (e) masking behavior of the free carrier absorption, (f) stabilizing action of the background screening, (g) saturation of absorption or amplification, and (h) effects of narrowing the semiconductor band gap and of changing the effective band gap of the superlattice [3–6]. Doping superlattices are feasible for integration in optical circuits and, moreover, a photonic crystal heterostructure (PCH) can be fabricated in a desirable manner to provide appropriate dispersion properties and optical spectra.

* Further author information: (Send correspondence to V.K.K.)
V.K.K.: E-mail: lavik@dragon.bas-net.by, Telephone: 375 17 2 840435
M.M.: E-mail: mmarcin@itl.waw.pl, Telephone: (+48 22) 812 00 72
D.V.U.: E-mail: ushakovdv@bsu.by, Telephone: 375 17 2 781313

Photonic Crystals and Fibers, edited by Waclaw Urbanczyk, Bozena Jaskorzynska, Philip St. J. Russell,
Proc. of SPIE Vol. 5950, 59500B, (2005) · 0277-786X/05/$15 · doi: 10.1117/12.622266

In previous works [7–9] we studied the possibilities to use *n–i–p–i* superlattices as optically controllable active layers in photonic band-gap structures. We considered a photonic structure in the GaAs-AlGaAs system where the absorption layers with optical controllable parameters were the GaAs *n–i–p–i* crystal layers. New types of laser microcavities based on δ-doped superlattices for providing the low-threshold lasing at multiple wavelengths and emission in opposite directions have been also proposed [10].

The development of various novel optoelectronic elements based on PCHs is of great interest. As an active medium with high optical nonlinearity, semiconductor doping superlattices of *n-i-p-i* crystal type have been advanced. Doping superlattices reveal optical and electric parameters that are compatible with optical and electronic integrated circuits. In particular, PCHs with active layers of doping superlattices can be proper selected for obtaining the required index contrast and for receiving the radiation emission in a wide spectral diapason [11].

Different PCHs composed of doping superlattices and wide-band-gap semiconductor layers are proposed and optimized. In the GaAs–GaInP system, laser sources, optical amplifiers, and switches are designed for the near-infrared region. Proposed PCH elements are well provided with the Al-free technology.

2. PHOTONIC HETEROSTRUCTURE DESIGN

For constructing a compositional photonic band-gap material, we suggest to use heterostructures in the GaAs-$Ga_xIn_{1-x}P$ system, which are lattice-matched to the GaAs substrate (Fig. 1). Each layer is characterized by the thickness d and complex, in general case, refractive index $n(\lambda) = n_r(\lambda) - i\kappa(\lambda)$ being a function of the light wavelength λ.. Active layers are made as the GaAs *n-i-p-i* crystals with δ-doped *n*- and *p*-layers of 2.8 nm-thickness and 5.3×10^{19} cm^{-3}-donor and acceptor concentrations and with *i*-layers of 11.3 nm-thickness. The active regions are controllable and their optical properties are modified under electric or optical excitation [2, 3]. The superlattice period is markedly smaller than the period of the photonic band-gap structure, therefore the approximation of the effective refractive index is applied for the description of the active medium optical properties. The refractive index n_r and coefficient of extinction κ of *n-i-p-i* superlattice layers depends on the light wavelength λ and difference in the quasi-Fermi levels ΔF [6]. Light is assumed propagating perpendicularly to the interfaces of layers.

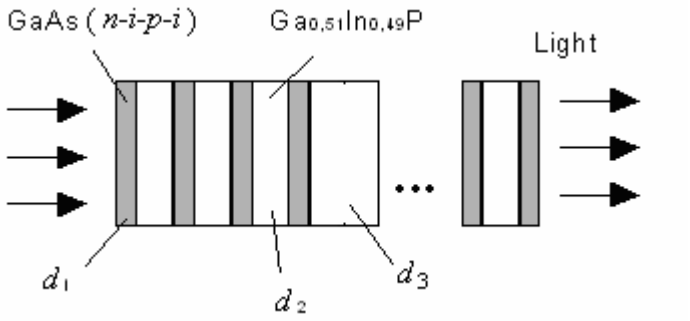

Figure 1. Schematic design of one-dimensional PCHs with the GaAs *n–i–p–i* crystal active layers. d_1 is the thickness of the GaAs superlattice, d_2 is the thickness of the GaInP passive layer component, d_3 is the thickness of the defect layer.

We consider the case, where the active layers of the PCH amplifier are uniformly excited by the electric or optical manner. Detail analysis of the output power performance and occurring nonlinear effects is carried out for one-dimensional PCH amplifiers having at the central part an active "defect" from the doubled GaAs *n-i-p-i* crystal. Passive components are 72,3 nm-thickness layers of a wide-gap semiconductor $Ga_xIn_{1-x}P$ with the mole fraction $x = 0.51$ and energy band gap of 1.89 eV. In the PCH amplifier under consideration, a doubled superlattice at the center offers an active defect component and the optical forbidden gap occurs at the wavelength region of 0.9 μm. In general, the input power P_{in} is assumed to be in the interval of 1 to 60 W/cm^2 and the dielectric function is calculated in dependence on ΔF. Since the gain saturation [12], the quantity of ΔF and refractive index n are changed from layer to layer and in the layers. The maximum variations are observed in the vicinity of the defect layer. The light field distribution in the PCHs is noticeably affected by dispersion parameters of the components and by conditions at the end faces [12, 13]. Gain saturation influences on the output in the reflection and transmission operations.

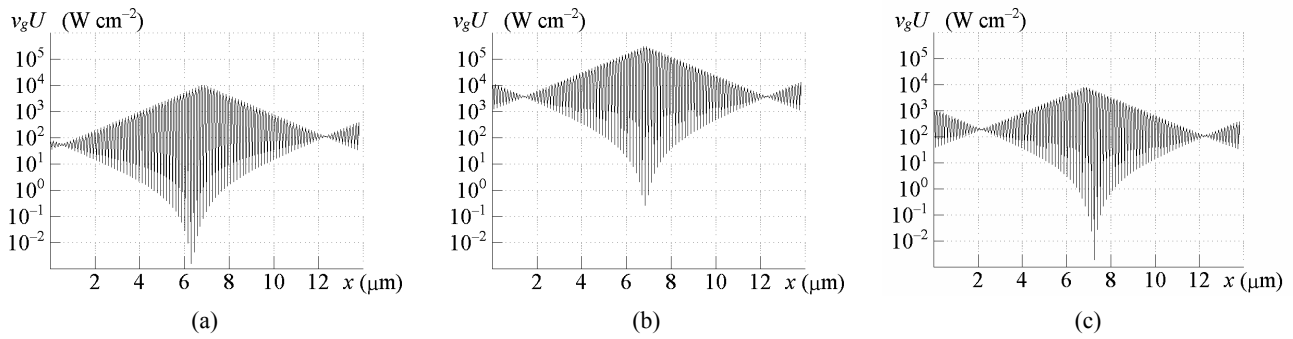

Figure 2. Spatial distribution of the intensity of radiation $v_gU(x)$ in the PCH at the defect mode wavelength λ_0 under different excitations of the active *n–i–p–i* layers (a) ΔF_0 = 1.37, (b) 1.41, and (c) 1.44 eV, the input radiation power P_{in} = 10 W/cm^2.

The self-consistent simulations of transmission and reflection spectra of the PCHs are performed using the transfer-matrix method and taking into account the saturation effects. These effects are mainly associated with the potential profile transformation in the superlattice layers at increasing the monochromatic radiation intensity and have principal influence on the spatial distribution of the electromagnetic field and respectively on the operating characteristics. The gain saturation in the active layers in the vicinity of the defect changes the index contrast of the PCH. It is attributed to the changes in the spatial distribution of the refractive index due to the nonlinear refraction [6, 12]. Symmetry in the distribution of the electromagnetic field is broken and a bundle near the input end face penetrates into the PCH volume (Fig. 2). So, changes in the index contrast of PCHs due to the gain saturation in the central defect amplifying layers makes worse the emission at the defect mode.

3. OPTICAL PROPERTIES OF PHOTONIC HETEROSTRUCTURES

The self-consistent calculations of the transmission and reflection spectra have been performed using the transfer-matrix method [9] and taking into account the saturation effects [5, 6, 12]. Saturation of the radiation absorption power in semiconductor low-dimensional crystals is connected with the energy subband filling by non-equilibrium current carriers [14]. As a result, the absorption coefficient k at a fixed light frequency ν decreases with increasing the electromagnetic wave intensity. This effect is associated with the approaching of the quasi-Fermi level difference ΔF to the photon energy $h\nu$ at increasing the monochromatic radiation intensity [15]. As found [5, 6], the absorption coefficient k of *n–i–p–i* crystals at the increase of the photon density S at a fixed frequency ν exhibits a non-monotonous behavior. The effect of "darkening", i. e., of the increasing k versus S occurs appreciably at photon energy values near the semiconductor band gap. The non-monotonous behavior of $k(S)$ results from redistribution of the subband levels, changes in the overlap integral of electron and hole wave functions at the potential profile transformation, and from the narrowing the effective band gap E_g' of the doping superlattice. The subband filling and emptying have also influence on the transmission and reflection characteristics of the PCH.

Quantitative description of the gain saturation and accompanying nonlinear refraction effects is carried out for one-dimensional PCH amplifiers having at the central part an active defect component from the doubled GaAs *n-i-p-i* crystal. For the first time, the nonlinear gain spectrum for δ-doped layer superlattices is calculated and changes in the refractive index within the photonic band gap of the PCH amplifiers are determined.

3.1. Saturation Process of Amplification

For the determining of the dependence of the gain coefficient on the density of energy of the electromagnetic field in every active *n-i-p-i* layer, the standard system of the stationary rate equations for non-equilibrium current carriers in the quantum wells of the superlattice potential relief and the photon density is used [6, 15]. The rate of generation (excitation) of current carriers is determined by the initial value of the quasi-Fermi difference ΔF_0 if the nonlinear effects are not essential and the radiation flux is negligible. The definite rate of spontaneous radiative recombination R_{sp0} corresponds to this value ΔF_0. In general case, the gain coefficient $k(\nu)$ in the active layers is related to the sum rate of radiative and non-radiative recombination R_{sp}/η_{sp} in a separate active layer and to the density of energy U of monochromatic

electromagnetic wave propagating in the PCH according to the expression $k(\nu) = h\nu\,(R_{sp0}/\eta_{sp0} - R_{sp}/\eta_{sp})/v_g\,U$. Here v_g is the group velocity of light, $h\nu$ is the photon energy, η_{sp} is the quantum yield of luminescence, The non-radiative recombination lifetime constant can be in particular taken equaled to $\tau_{nr} = 1$ μs.

At sufficiently high U, the gain coefficient is inverse proportional to the light flux. Then, introducing the initial gain coefficient k_0, we obtain $k = k_0/\alpha_\infty U$, where the nonlinearity parameter $\alpha_\infty = v_g\,k_0/h\nu\,(R_{sp0}/\eta_{sp0} - R_{sp}/\eta_{sp})$. Here R_{sp} corresponds to $\Delta F \approx h\nu < \Delta F_0$. In general case, the gain saturation is described by the law $k = k_0/(1 + \alpha U)$, where $\alpha \le \alpha_\infty$ [12]. Features of nonlinear gain and absorption in injection lasers are established by analogous way [15].

The nonlinearity parameter α in dependence on the radiation density in active *n-i-p-i* layers can be of different values. At low light fluxes, $\alpha = \alpha_0$ and the gain saturation follows to the expression $k = k_0(1 - \alpha_0 U)$. For middle values of the radiation density U, where k drops at two times, it is necessary to use the quantity $\alpha = \alpha_{1/2}$. At high U, the nonlinearity parameter is $\alpha = \alpha_\infty$. Herewith, the relation $\alpha_0 < \alpha_{1/2} < \alpha_\infty$ is fulfillment [12].

Results of calculations [12] of the gain spectrum and dependence $k(U)$ in *n-i-p-i* layers at the temperature $T = 300$ K is presented in Fig. 3. The nonlinearity parameter α decreases monotonically with the radiation wavelength λ and at the twofold drop of the gain coefficient with the increasing of U the corresponding value $\alpha_{1/2}/v_g$ in the wavelength interval 0.90-0.97 μm is $(3.42\text{-}0.99)\times10^{-6}$ cm^2/W.

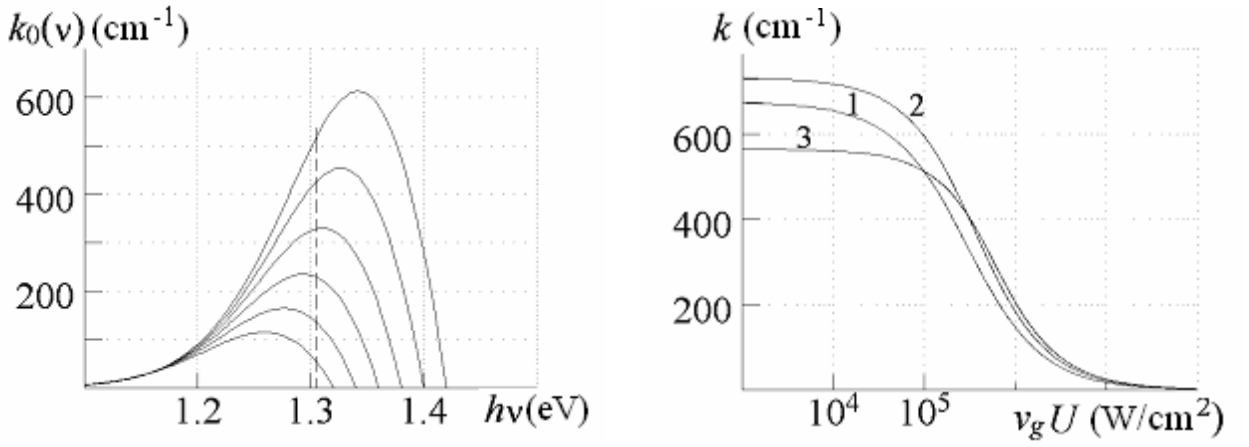

(a) (b)

Figure 3. (a) Gain spectrum $k_0(\nu)$ at different excitation levels ΔF_0 in *n-i-p-i* layers and (b) saturation curves $k(U)$ at different wavelengths and $\Delta F_0 = 1.435$ eV. Numbers at the curves (b) correspond to (1) $\lambda = 900$, (2) 920, and (3) 950 nm, the value ΔF_0 coincides with the intersection of the curves (a) with the abscissa, the dash line shows the defect mode position.

3.2. Resonance of Transmission and Reflection Spectra

Two new nonlinear optical effects in the PCHs with active *n-i-p-i* layers are predicted [16]. One effect is related with the appearing of two neighboring resonance peaks of the output power in both reflection and transmission operation at the defect mode versus the pump level of the *n-i-p-i* layers (Fig. 4). The pump level of the active component layers is characterized by the initial value of the quasi-Fermi level difference $\Delta F = \Delta F_0$ or by the current density j at electric excitation. Similar behavior is obtained in dependence on the input radiation power P_{in} (Fig. 5).

The maximum wavelength λ_0 of the transmission and reflection spectra shifts to the short-wavelength region with increasing ΔF. Near $\Delta F = 1.41$ eV two subsequent drops of λ_0 occur. As a result, two peaks in the dependencies $T_0(\Delta F)$ and $R_0(\Delta F)$ appear. The highest values of the transmission T_0 and reflection R_0 coefficients reach up to 400 at $P_{in} = 10$ W/cm^2. The response at the defect mode decreases with further increasing the input power P_{in}.

Another effect is bistable switching in the transmission and reflection at the spectral tuning within the defect mode band. The tuning can be realized with increasing or decreasing the signal wavelength λ. The responses in these regimes differ that reflects as hysteresis. The width of the spectral hysteresis loop depends on the input signal intensity and pump.

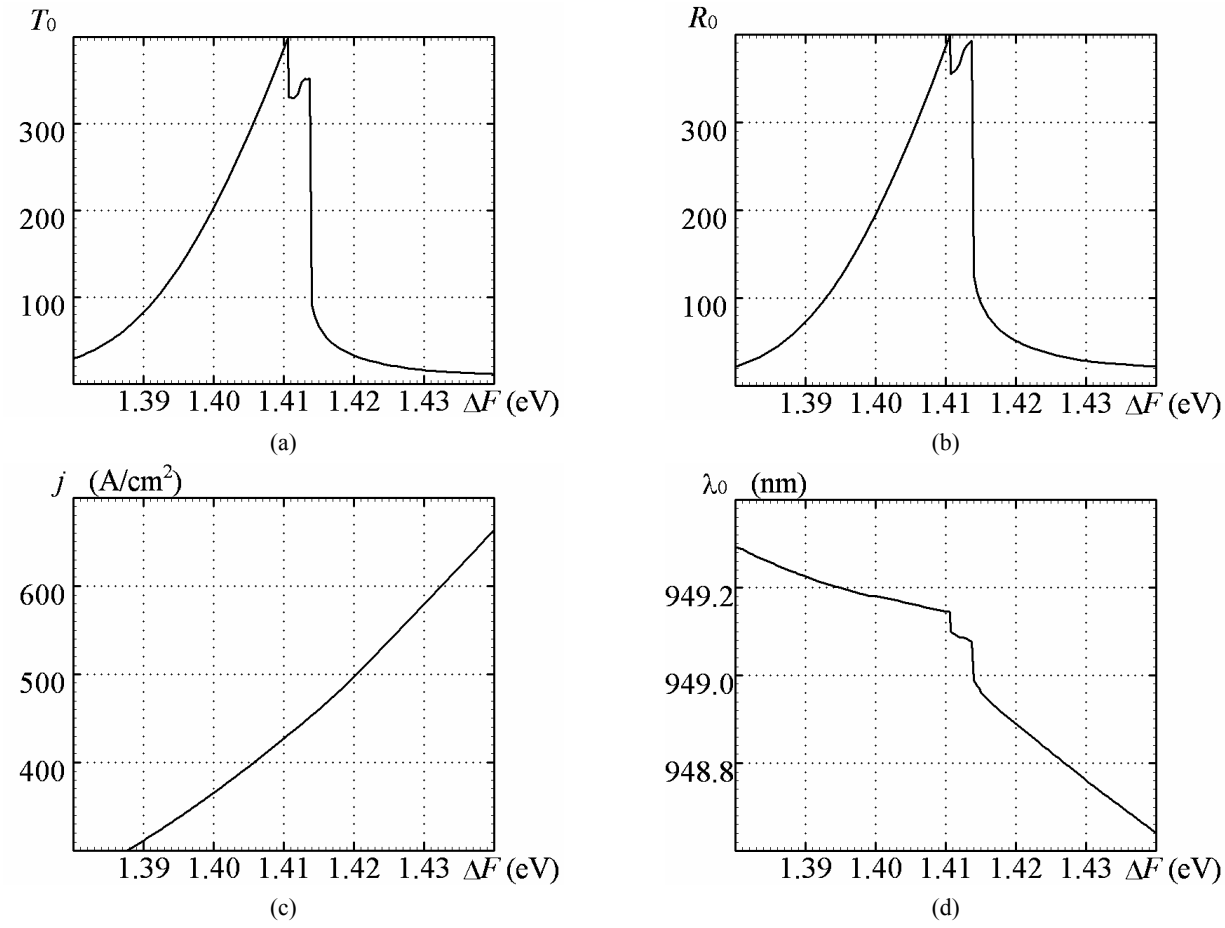

Figure 4. (a) Transmission T_0 and (b) reflection R_0 coefficients of the PCH with *n-i-p-i* active layers corresponding to the maximum wavelength λ_0 of the spectra versus the quasi-Fermi level difference $\Delta F = \Delta F_0$, (c) the relation between the current density j and the difference ΔF in the active layers, and (d) shift of λ_0 with the increasing of ΔF, P_{in} = 10 W/cm^2.

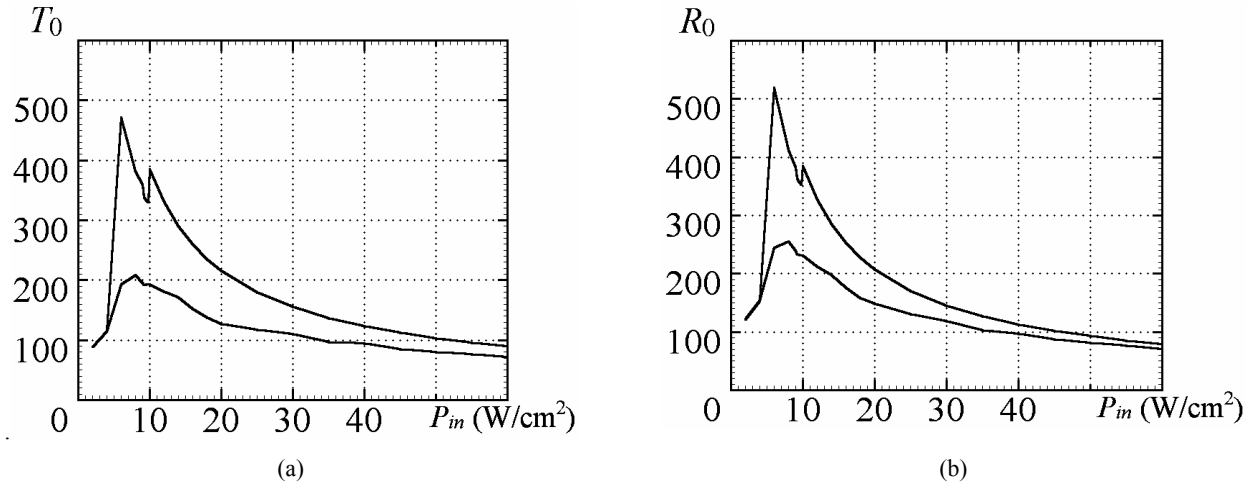

Figure 5. (a) Transmission T_0 and (b) reflection R_0 coefficients of the PCH with *n–i–p–i* active layers corresponding to the maximum wavelength λ_0 of the spectra versus the input power P_{in}. ΔF_0 = 1.41 eV.

It is seen from Fig. 5 (the overhead curves are obtained for the increasing of λ) that on the dependence of maximum transmission T_0 and reflection R_0 coefficients on the input radiation power P_{in} two adjacent maxima are also observed. The highest values of the transmission T_0 and reflection R_0 coefficients are, accordingly, 460 and 520 at the input power P_{in} = 6 W/cm^2. The bottom curves in Fig. 5 correspond to values of maximum transmission and reflection spectra which are received in the regime of the decreasing of λ.

3.3. Spectral Bistability and Hysteresis Behavior

The bistability in the transmission and reflection spectra is pronounced near the defect mode. Changes in the refractive index which result from the gain saturation are responsible for respective changes in the PCH transmission spectrum. In general, a positive (negative) nonlinearity has a tendency to shift respectively the entire transmission spectrum to the left (right). Specially, when the resonance is sharp enough, bistability or multistability can be achieved [17]. For a pure periodic structure, the bistability usually occurs near the resonance peak at the border of the photonic band gap.

As an example, we display in Figs. 6 and 7 the transmission spectra of the PCH with active *n–i–p–i* layers in the vicinity of the defect resonance peak located in the basic photonic band gap. Each spectrum is calculated using a fixed input power P_{in} or quasi-Fermi level difference ΔF_0. Near a certain threshold P_{in} or ΔF_o, the spectrum exhibits the bistability phenomenon. In particular, decreasing the wavelength of a tunable source results in the transmission jump into high-transmission state 1' after passing point 1. Similarly, the low-transmission state 2' can be reached after passing state 2 when moving in the opposite spectral direction (Fig. 6).

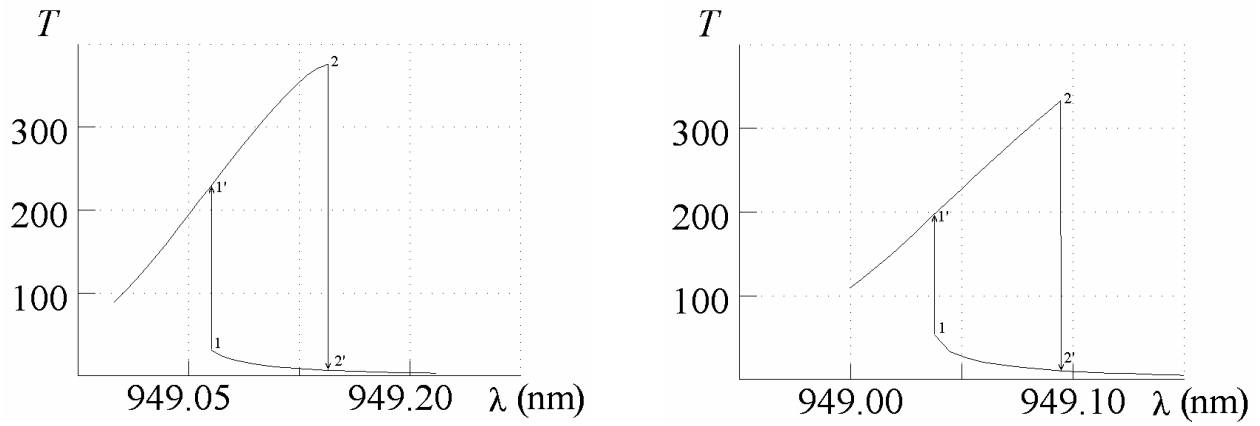

Figure 6. Hysteresis of the transmission spectra $T(\lambda)$ in the defect mode bandwidth at different initial values of the quasi-Fermi level difference (a) ΔF_0 = 1.410 and (b) 1.411 eV. P_{in} = 10 W/cm^2.

Transformation of the transmission spectrum hysteresis curves with growth of an input power is shown in Fig. 7. At small values of an input power less than 4 W/cm^2 the spectral hysteresis in the defect mode region is not manifested. In this case, both curves $T_0(P_{in})$ coincide and the hysteresis at the tuning of λ is not observed (Fig. 7 a). At high powers both curves approach asymptotically to each other (see Fig. 5 a) and the hysteresis loop becomes less pronounced.

Changes in the reflection spectrum $R(\lambda)$ of the PCH in dependence on the input power P_{in} are shown in Fig. 8. The amplitude of the defect mode follows non-monotonically with the input radiation intensity and is also determined by the course of tuning the wavelength (increasing or decreasing λ near the defect mode). For the curves corresponding to the increasing of λ, in the reflection operation two adjacent maxima of $R(\lambda) \approx 500$ are observed at P_{in} = 6 and 10 W/cm^2.

Switching behavior in output power operation at a fixed wavelength of input light intensity is demonstrated in Fig. 9. Output–input characteristics of specific S-type appear only in a narrow spectral interval near the defect mode. This interval overlaps only 0.2 nm that is related to the PCH design and is obviously determined by the number of periods of photonic structure [18].

The output–input characteristics of the PCH depends on the tuning of the signal wavelength out the defect mode. When the input power P_{in} increases up to a switching threshold value, the output power P_{out} jumps to a higher value (from state 1 to state 1'). Then, P_{out} increases monotonously versus the value of P_{in}. On the other hand, when P_{in} decreases from the value that is greater than the threshold value, P_{out} decreases slowly until it reaches state 2 at which it jumps to state 2'. Then, P_{out} continues to decrease monotonously with the decreasing of P_{in}. It is clearly seen that the hysteresis loop width depends markedly on the signal wavelength detuning.

It should be noticed that the region between the low-output state and high-output state, i. e., lines 1–1' and 2–2' correspond to unstable conditions. The higher switching threshold value (61 W/cm^2) and respectively larger unstable power region is observed at the defect resonance wavelength ($\lambda = 949.12$ nm) (curve 4 in Fig. 9). The switching threshold value can be reduced by the detuning of the wavelength of the input signal. For example, the switching threshold at $\lambda = 949.05$ nm is 11 W/cm^2 (curve 2 in Fig. 9). However, the bistable behavior can not be obtained if the input signal wavelength is not close to the defect resonance peak.

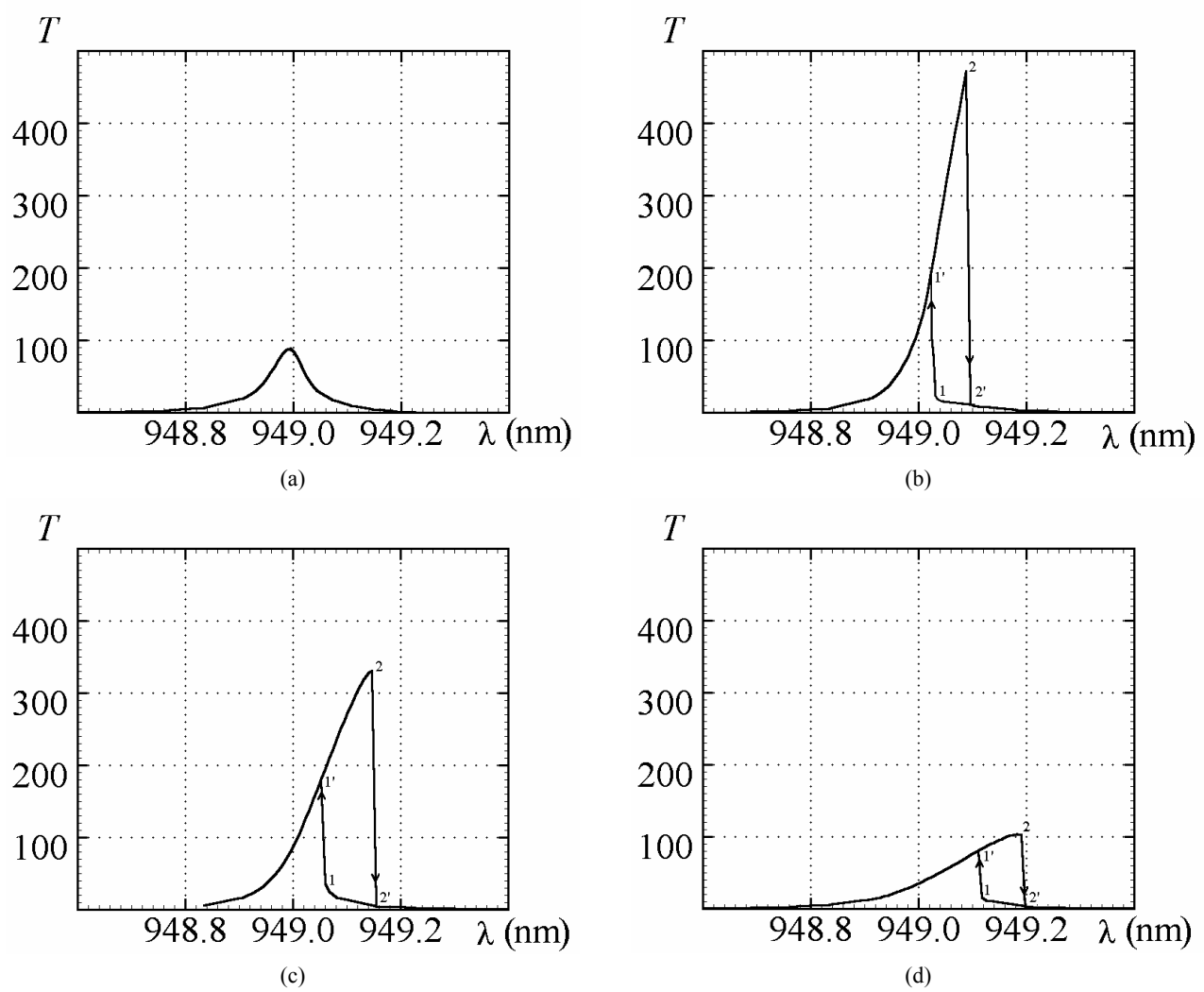

Figure 7. Hysteresis of the transmission spectra $T(\lambda)$ in the defect mode bandwidth at different values of the input power (a) $P_{in} = 2$, (b) 6, (c) 12, and (d) 50 W/cm^2. $\Delta F_0 = 1.41$ eV.

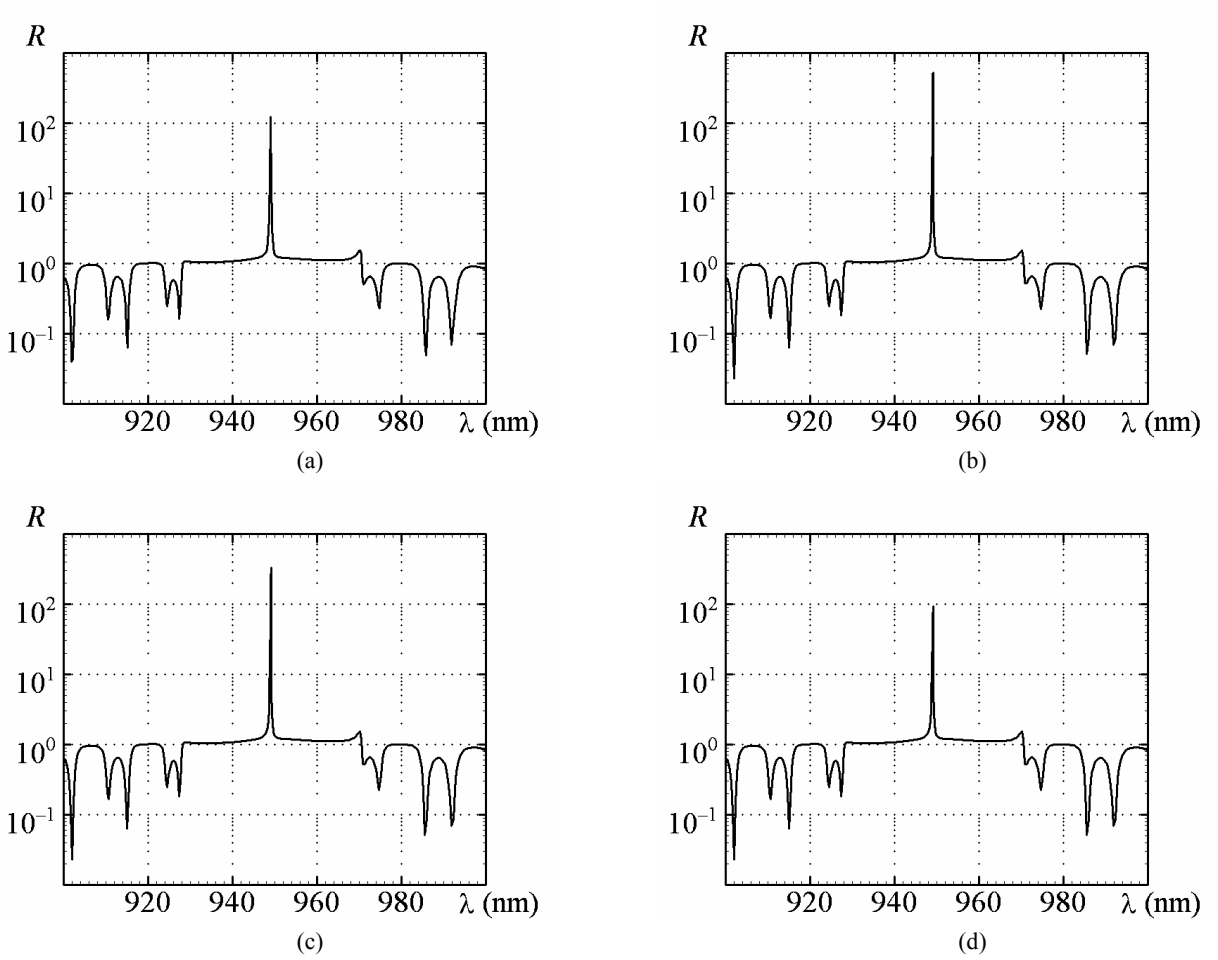

Figure 8. Reflection spectrum $R(\lambda)$ of the PCH in the region of the photonic band-gap including the defect mode in the center at different values of the input power (a) $P_{in} = 2$, (b) 6, (c) 12, and (d) 50 W/cm^2, $\Delta F_0 = 1.41$ eV.

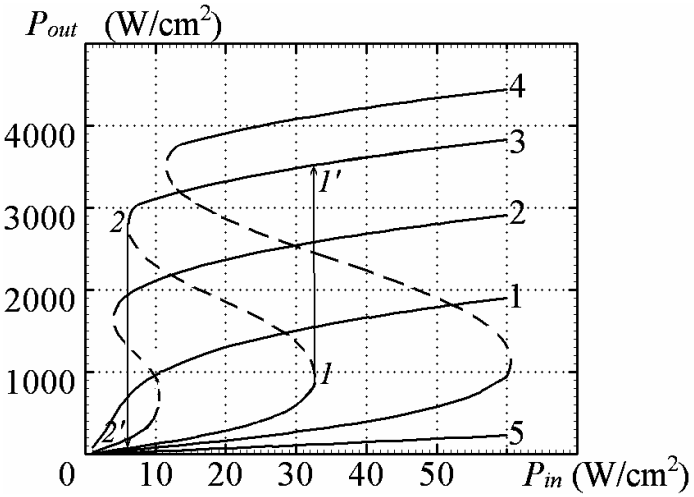

Figure 9. Output–input characteristics of the PCH at different wavelengths (1) λ = 949.00, (2) 949.05, (3) 949.10, (4) 949.12, and (5) 949.20 nm, $\Delta F_0 = 1.41$ eV.

4. CONCLUSION

Different PCHs composed of doping superlattices and wide-band-gap semiconductor layers are designed. Proposed in the GaAs–GaInP system laser sources, optical amplifiers, and switches are attractive for the near-infrared region. The self-consistent simulation of optical effects is carried out for one-dimensional PCH amplifiers having at the central part an active defect from the doubled GaAs *n-i-p-i* crystal. For the first time, the nonlinear gain spectrum for δ-doped superlattices is calculated and the accompanying changes in the refractive index within the photonic band gap of the PCH are determined. The effects are mainly associated with the potential profile transformation in the superlattice layers at increasing the monochromatic radiation intensity and have principal influence on the spatial distribution of the electromagnetic field and respectively on the PCH operating characteristics.

Two new nonlinear optical effects in the PCHs with active *n-i-p-i* layers are predicted. One effect is related with the appearing of two neighboring resonance peaks of the output power in both reflection and transmission operation at the defect mode versus the pump level of the *n-i-p-i* layers. Another effect is bistable switching in the transmission and reflection at the spectral tuning within the defect mode band. The width of the spectral hysteresis loop depends markedly on the input signal intensity and on the active layer pump. Spectral switching and modulation of transmission and reflection spectra of the PCHs occur for the response times shorter than ≈ 10 ps. It shows potential opportunities of the PCHs with active *n–i–p–i* layers as high-speed optical amplifiers and switches.

ACKNOWLEDGMENTS

One of the authors (VKK) is mainly thankful the National Institute of Telecommunications, Warsaw, for supporting during the SPIE-COO, hospitality, and fruitful collaboration.

REFERENCES

1. H. Ando. H. Iwamura, H. Oohashi, and H. Kanbe, "Nonlinear absorption in *n–i–p–i* MQW structures," *IEEE J. Quantum Electron*. **25**, pp. 2135–2141, 1989.
2. G. H Dohler, "Non-linear optical properties of *n–i–p–i* and hetero *n–i–p–i* structures and their potential for applications in photonics," *Opt. & Quantum Electron*. **22**, pp. S121–S140, 1990.
3. V. K. Kononenko, I.S. Manak, and D.V. Ushakov, "Optoelectronic properties and characteristics of doping superlattices," *Proc. SPIE*. **3580**, pp. 10-27, 1998.
4. D. V. Ushakov, V. K. Kononenko, and I. S. Manak, "Effects of energy spectrum broadening in doping semiconductor superlattices," *J. Appl. Spectrosc*. **66**, pp. 820–825, 1999.
5. D. V. Ushakov, V. K. Kononenko, and I. S. Manak, "Saturation of absorption in *n–i–p–i* crystals," in *Proc. SPIE.* **4358**, pp. 171–174, 2001.
6. D. V. Ushakov, V. K. Kononenko, and I. S. Manak, "Nonlinear optical properties in semiconductor doping superlattices," *J. Appl. Spectrosc.* **68**, pp. 656–662, 2001.
7. V. K. Kononenko., D. V. Ushakov., I. S. Nefedov, V. N. Gusyatnikov, and Yu. A. Morozov, "Control of transmission in photonic structures with *n-i-p-i* layers," in *Proc. 3rd Int. Workshop on Laser and Fiber-Optical Modeling*, pp. 97–99, Kharkiv, 2001.
8. V. N. Gusyatnikov, I. S. Nefedov, Yu. A. Morozov, V. K. Kononenko, and D. V. Ushakov, "Controllable one-dimensional photonic structures with *n–i–p–i* crystal layers," in *Physics, Chemistry and Application of Nanostructures*, pp. 142–145, World Scientific, Singapore, 2001.
9. I. S. Nefedov, V. N. Gusyatnikov, M. Marciniak, V. K. Kononenko, and D. V. Ushakov, "Optical gain in one-dimensional photonic band gap structures with *n–i–p–i* crystal layers," *J. Telecommun. Information Technol*. 1, pp. 60–64, 2002.
10. A. G. Smirnov, D. V. Ushakov, and V. K. Kononenko, "Multiple-wavelength lasing in one-dimensional bandgap structures: implementation with active *n–i–p–i* layers," *J. Opt. Soc. Am. B* **19**, pp. 2208–2214, 2002.
11. V. K. Kononenko, D. V. Ushakov, and A. G. Smirnov, "Photonic crystal heterostructures with controllable active layers," in *Proc. ICTON* **1**, pp. 247–251, Warsaw, 2003.
12. V. K. Kononenko, A. G. Smirnov, and D. V. Ushakov, "Influence of gain saturation on output power characteristics of the photonic crystal type heterostructures," *Bull. RAS* **68**, pp. 127–130, 2004.

13. D. V. Ushakov, V. K. Kononenko, and A. G. Smirnov, " Amplification in photonic crystal heterostructures with active media from doping superlattice layers," in *Proc. 4th Int. Workshop on Laser and Fiber-Optical Modeling*, pp. 159–161, Kharkiv, 2002.
14. V. K. Kononenko, "Nonlinear absorption in quantum-size heterostructures," *Phys. stat. sol. (b)* **150**, pp. 695-698, 1988.
15. V. K. Kononenko and V. P. Gribkovskii, "Effect of saturation in semiconductor light amplifiers and filters," *Opt. & Spectrosc*. 2**9**, pp. 975–984, 1970.
16. D. V. Ushakov, M. Marciniak, and V. K. Kononenko, " Nonlinear optical effects in one-dimensional photonic crystal heterostructure amplifiers," in *Proc. ICTON* **1**, pp. 330–332, 2003.
17. V. M. Agranovich, S. A. Kiselev, and D. L. Mills, "Optical multistability in nonlinear superlattices with very thin-layers," *Phys. Rev. B* **44**, pp. 10917–10920, 1991.
18. Y.-C. Tsai, K. W.-K. Shung, and S.-C. Gou, "Impurity modes in one-dimensional photonic crystals-analytic approach," *J. Mod. Opt.* **45**, pp. 2147–2157, 1998.